Multi-Resolution and Noise-Resistant Surface Defect Detection Approach Using New Version of Local Binary Patterns

Shervan Fekri-Ershad & Farshad Tajeripour

Taylor & Francis
Taylor & Francis Group

Check for updates

Multi-Resolution and Noise-Resistant Surface Defect Detection Approach Using New Version of Local Binary Patterns

Shervan Fekri-Ershad[a,b] and Farshad Tajeripour[c]

[a]Faculty of Computer Engineering, Najafabad Branch, Islamic Azad University, Najafabad, Iran; [b]Big Data Research Center, Najafabad Branch, Islamic Azad University, Najafabad, Iran; [c]Department of Computer Science and Engineering, Shiraz University, Shiraz, Iran

ABSTRACT

Visual quality inspection systems play an important role in many industrial applications. In this respect, surface defect detection is one of the problems that have received much attention by image processing scientists. Until now, different methods have been proposed based on texture analysis. An operation that provides discriminate features for texture analysis is local binary patterns (LBP). LBP was first introduced for gray-level images that makes it useless for colorful samples. Sensitivity to noise is another limitation of LBP. In this article, a new noise-resistant and multi-resolution version of LBP is used that extracts color and texture features jointly. Then, a robust algorithm is proposed for detecting abnormalities in surfaces. It includes two steps. First, new version of LBP is applied on full defect-less surface images, and the basic feature vector is calculated. Then, by image windowing and computing the non-similarity amount between windows and basic vector, a threshold is computed. In test phase, defect parts are detected on test samples using the tuned threshold. High detection rate, low computational complexity, low noise sensitivity, and rotation invariant are some advantages of our proposed approach.

Introduction

Any hole, damage, abnormalities, and slot in product surfaces are called defect (Tajeripour and Fekriershad 2014). Defects on product surfaces affect quality. The main aim of visual quality inspection systems (VQIS) is detecting abnormalities in surface images. VQIS can be used in many industrial applications such as tiles, metal, agricultural products, fabric, and paper. Until now, many different methods have been proposed to do this task. State-of-the-art approaches can be categorized in three categories as: Spatial Domain, Frequency Domain, and Joint Domains.

For instance, Henry, Grantham, and Nelson (2010) proposed an approach in (Henry, Grantham, and Nelson 2010) based on ellipsoidal region features and min-max technique. It was evaluated on patterned fabrics to detect defect parts automatically. It can be categorized in spatial domain.

Threshold is one of the common methods to separate objects from background in VQIS. In (Yuan, Wu, and Peng 2015), an improved extension of Otsu threshold is proposed for surface defect detection. Their proposed approach is weighting object variance in unimodal or bimodal histograms of input images. This approach is run in spatial domain. As a recent work, in (Lin and Yu-Yeh 2009), a texture defect detection system is described based on image deflection compensation. A general surface defect detection method is proposed in (Fekriershad and Tajeripour 2012), which is invariant with respect to texture descriptor. They proposed a one-dimensional version of local binary patterns to detect defects on fabric textile and stone surfaces.

Ghazini, Monadjemi, and Jamshidi (2009) proposed a defect detection approach of tiles using combination of wavelet transform and statistical features. It is evaluated in frequency domain. In (Tolba 2011), a probabilistic neural network (PNN) is used for fast defect classification based on the maximum posterior probability of the Log-Gabor based statistical features. In (Harinath et al. 2015), authors extracted some wavelet features to identify images. Then a genetics-based algorithm is proposed for fabric defect detection based on shanon entropy. Alimohamadi and Ahmady (2008) proposed a new method using optimal Gabor filters to detect skin defect of fruits that was usable in agricultural products visual quality inspection systems (APVQIS). Some researchers try Fourier transform to achieve this aim. For example, in (Chan and Pang 2000), Chan and Pang proposed a robust approach for fabric textile defect detection by Fourier analysis. They defined a diagram, which is called central spatial frequency spectrum, to analyse an image. A review paper about defect detection approaches is proposed in (Xie 2008).

The mathematical/computational complexity of some previous approaches is high, and some of them don't guarantee an accurate result for every kind of surfaces. Noise and rotation sensitivity can be mentioned as big limitations of many state-of-the-art approaches. The main aim of this article is to propose an approach for surface defect detection that satisfies mentioned limitations.

LBP is a non-parametric operator that describes the local spatial structure and local contrast of an image. Previous researches show its power to extract discriminate features to distinguish and identify surfaces.

In this article, first, a noise-resistant and multi-resolution version of LBP is proposed that extracts color/texture features jointly. It is called Noise-resistant Color Local Binary Patterns (NrCLBP). Next, a novel approach is proposed for detecting surface defects using NrCLBP. The proposed approach detection algorithm includes two phases. In the first phase, some surely defect-less images were taken and analyzed by NrCLBP operator, and a basic feature vector is

extracted, which is a good identification for non-defects parts. Then, by using image windowing technique and Log-Likelihood ratio, an accurate threshold is computed for defect-less image. In the second phase, by extracting NrCLBP features of test images and comparing them with extracted basic feature vector, defect parts are detected. In the result part, two experiments are evaluated on two different databases that include fabric textile surface and stone surface images. High detection rate in comparison with other state-of-the-art methods shows the quality of the proposed approach. Low computational complexity, rotation invariant, illumination invariant, noise resistance, and multi-resolution are some other advantages of the proposed approach.

Article organization

The article is organized as follows: In section 'local binary patterns (LBP)', first, basic theory of LBP is discussed as a texture descriptor. Then modified version of LBP is survived. In section 'Noise-resistant color LBP', our proposed noise-resistant and multi-resolution texture analysis operation is described, which extracts color/texture features jointly. Section 'Proposed surface defect detection approach', presents our proposed surface defect detection algorithm with details. Experimental results are included in section 'Results'. Finally, the 'Conclusion' is presented as the last section.
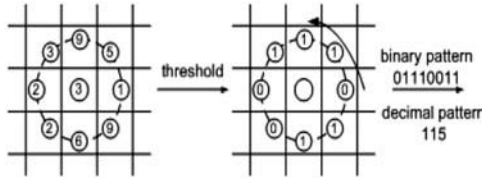
Local binary patterns

Local binary pattern (LBP) was originally proposed in (Ojala, Maeenpaeae, and Pietikaeinen 2000) for the first time. LBP is an texture analysis operator that describes the local contrast and local spatial structure of an image. To evaluate the LBP, at a given pixel position (x_c, y_c), LBP is described as an ordered set of binary comparisons of pixel intensities between the center pixel and its neighbors. Neighborhoods could be assumed circular because of achieving the rotation invariant. Points that the coordinations are not exactly located at the center of pixel would be found by bilinear interpolation. LBP is defined as follows:

$$\mathbf{LBP_{P,R}} = \sum_{k=1}^{P} \phi(g_k - g_c)2^{k-1} \tag{1}$$

Where "g_c" corresponds to the gray value of the centered pixel and "g_k" to the gray values of the neighborhood. P will be the number of neighborhoods, and function $\phi(x)$ is defined as:

$$\phi(\mathbf{x}) = \begin{cases} 1 \ if \ x \geq 0 \\ 0 \ else \end{cases} \tag{2}$$

Figure 1. An example of applying LBP with P = 8 and R = 1.

An example of applying $LBP_{8,1}$ operator is shown in Figure 1.

The $LBP_{P,R}$ operator produces (2^P) different output values, corresponding to the 2^P different binary patterns that can be formed by the P pixels in the neighbor set. When the image is rotated, the gray values "g_k" will correspondingly move along the perimeter of the circle around "g_c." To remove the effect of rotation, that is, to assign a unique identifier to each rotation, invariant local binary patterns is defined:

$$\mathbf{LBP_{P,R}^{ri}} = \min\left\{\mathrm{ROR}\left(\mathrm{LBP}_{P,R}, \beta\right)|\beta = 0, 1, \ldots, p-1\right\} \tag{3}$$

Where "ri" means rotation invariant and ROR(x, β) performs a circular bitwise rotate right on the P-bit number x, β times. Finally, the minimum of computed values for β = 0 to p-1 would be chosen.

Modified local binary patterns (MLBP)

Practical experience of the authors in (Pietikäinen, Ojala, and Xu 2000) has shown that LBP doesn't provide very good discrimination, and the computation complexity is high. To solve these problems, Ojala, Pietikainen, and Maenpaa (2002) proposed a new version of LBP that is known as modified local binary patterns (MLBP). They (2002) defined a uniformity measure "U," which corresponds to the number of spatial transitions (bitwise 0/1 changes) in the "pattern." It is shown in Equation 4. For example, pattern 11111111 has U value of 0, while 11001001 has U value of 3.

$$\mathbf{U\left(LBP_{P,R}\right)} = \left|\phi\left(g_1 - g_c\right) - \phi\left(g_p - g_c\right)\right|$$
$$+ \sum_{k=2}^{p}\left|\phi\left(g_k - g_c\right) - \phi\left(g_{k-1} - g_c\right)\right| \tag{4}$$

Applying MLBP, the patterns that have uniformity amount less than U_T are grouped as uniform patterns, and the patterns with uniformity amount more than U_T are grouped as non-uniform patterns. Finally, the LBP is computed as follows.

$$LBP_{P,R}^{riu_T} = \begin{cases} \sum\limits_{k=1}^{P} \phi(g_k - g_c) & \text{if } U(LBP_{P,R}) \leq U_T \\ P+1 & elsewhere \end{cases} \quad (5)$$

"riu_T" reflects the use of uniform threshold. Applying $LBP_{P,R}^{riu_T}$ will assign a label from 0 to P to uniform patterns and label $P + 1$ to non-uniform patterns. In using $LBP_{P,R}^{riu_T}$ just one label $(P + 1)$ is assigned to all of the non-uniform patterns. To achieve discriminative features, U_T should be optimized that uniform labels cover majority patterns in the image. Recent researches (Fekriershad and Tajeripour 2012; Tajeripour and Fekriershad 2014, 2012; Tajeripour, Kabir, and Sheikhi 2008) show that if the value of U_T is selected equal to (P/4), only a negligible portion of the patterns in the texture takes label P + 1. $LBP_{P,R}^{riu_T}$ quantifies the occurrence statistics of individual rotation invariant patterns corresponding to certain micro-features in the image, and hence the patterns can be considered as feature detectors. For example, Figure 2 illustrates the 36 unique rotation invariant local binary patterns that can be occurred in the case of P = 8 and R = 1. For example, pattern #0 detects bright spots, #8 dark spots or flat areas, #4 edges, and so on.
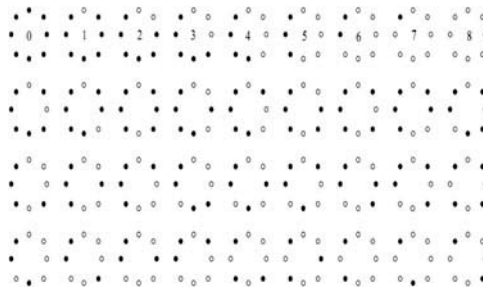
(a) Hatchet Stone (b) Orange Travertine Stone (c) Creamy Travertine Stone

(d) Box Pattern Fabric (e) Star Pattern Fabric (f) Dot Pattern Fabric

One label is assigned to each neighborhood. So, a feature vector like D can be extracted for each image as follows:

$$D = <d_0, d_1, ..., d_{P+1}> \quad (6)$$

Where:

$$d_k = \frac{N_k}{N_{total}} \quad 0 \leq k \leq P+1 \quad (7)$$

Figure 2. The 36 unique rotation invariant binary patterns that can occur in the circularly symmetric neighbor set of $LBP_{8,R}$. Black and white circles correspond to bit values of 0 and 1 in the output (a) Hatchet Stone (b) Orange Travertine Stone (c) Creamy Travertine Stone (d) Box-Pattern Fabric (e) Star-Pattern Fabric (f) Dot-Pattern Fabric.

N_k shows total number of neighbors that is labeled as K, and N_{total} is the size of input image. finally, extracted vector has $P + 2$ dimensions. d_k is the occurrence probability of label k in whole. To obtain d_k, first $LBP_{P,R}^{riu_T}$ should be applied on the whole image, and the labels are assigned to neighbors. Then the occurrence probability of each label in the image is regarded as one of the dimensions of the feature vector.

Noise-resistant Color LBP (NrCLBP)

The basic LBP scheme and most of its improved versions such as MLBP (Ojala, Pietikainen, and Maenpaa 2002), MBP (Hafiane, Seetharaman, and Zavidovique 2007), and LTP (Tan and Triggs 2010) were defined for grayscale images. We propose a simple extension to color images. The proposed descriptor is invariant with respect to several transformations in the color spaces. Color images can be represented in different color spaces such as RGB, HSV, and YC_bC_r. In this part, the definition is evaluated in RGB. RGB uses an additive color mixing model of red, green, and blue colors. To represent color images, separate red, green, and blue components must be specified for each pixel, and so the pixel value is actually a vector of three numbers, which are known as g_r, g_g, g_b. Often the three different components are stored as three separate "grayscale" images known as *color planes* that have to be recombined when processing.

To combine color and texture information, each colorful input texture can be separated in three different color spaces. Now, the proposed texture analysis operator (Equation 6) can be computed for each color plans separately. Finally, the extracted vectors can be concatenated in a simple representation as follows:

$$D = <\ D_R,\ D_G,\ D_B>$$ (8)

Where D_R shows the extracted feature vector for color plane red using Equation 6. Also, D_G and D_B can be defined in a similar ways. Finally, vector D has 3P+6 dimensions.

Noise resistant

Image noise is random variation of brightness or color information in images and is usually an aspect of electronic noise. Noise produces undesirable effects such as artifacts, unrealistic edges, unseen lines, corners, blurred objects, and disturbed background. In this respect, different noise models can be defined such as Gaussian, white, Browning, impulse valued, periodic, and quantization. Impulse noise is seen in data transmission. Some image pixel values are replaced by corrupted pixel values. Impulse noise sensitivity is one of the big limitations of the LBP that decreases the analysis accuracy.
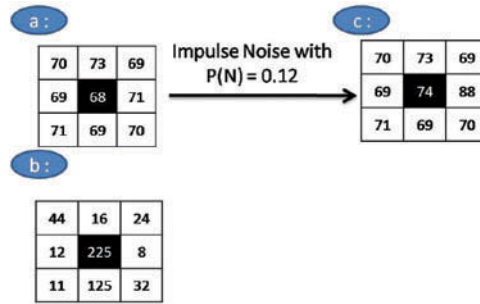
Figure 3. Noise effects on MLBP.

Even a small noise may change the LBP code significantly. In the evaluation of $LBP_{P,R}^{riu_T}$, threshold is considered at exactly the value of the central pixel, so LBP tends to be sensitive to noise, especially in near uniform image regions. It causes change label of the desired centered pixel that has effects on final extracted feature vector. Take the example of two different local neighbors as shown in Figure 3a and Figure 3b.

An impulse noise is applied on Figure 3a, and the output is shown in Figure 3c. The extracted labels for each pattern are as follows:

$LBP_{8,1}(a) = 8$ $LBP_{8,1}(b) = 0$ $LBP_{8,1}(c) = 0$

Figure 3a shows a local flat area, and Figure 3b shows a local bright spot. As a human visual inspection result, Figure 3c shows flat area, and it is more similar to Figure 3a, but its LBP label is same with Figure 3b. In this section, we propose an impulse noise-resistant version of LBP. The texture analysis techniques discussed above (Basic LBP, MLBP) had been defined for grayscale images. We proposed a simple extension of this technique to color images 'Noise resistant color LBP'. In a gray-level image like G, impulse noise can be defined as transmission function like N that probability changes some of the image pixel values as follows. Where G' shows the output noisy image.

$$G(x, y) \pm N(x, y) = G'(x, y) \qquad (9)$$

The noise occurrence probability on a specific pixel at given position (x,y) can be considered as P(N). In a colorful image with "i" color planes, at a given pixel position (x, y), impulse noise can be defined as follows:

$$G(x, y, i) \pm N(x, y, i) = G'(x, y, i) \qquad (10)$$

In a colorful image with a specific color space such as RGB, noise may be not occured in all color planes jointly. It may be occurred in a specific color planes. It means noise may disturb the pixel intensity in a specific color plane with probability of P(N)/3. It means that pixel values of a given pixel at

position (x, y) may not change at least in one of the color planes. To assume this mention, function $\Omega(x)$ can be newly defined as follows:

$$\Omega_X = \begin{cases} 1 \ if \ (\Omega_{X_R} \times \Omega_{X_G} \times \Omega_{X_B}) = 1 \\ 0 \ if \ (\Omega_{X_R} \times \Omega_{X_G} \times \Omega_{X_B}) = 0 \end{cases} \tag{11}$$

Where

$$\Omega_{X_i} = \begin{cases} 1 \ if \ \left(f'_{i_k} - f'_{i_c}\right) > 0 \\ 0 \ else \end{cases} \tag{12}$$

Where G'_{i_c} corresponds to the gray value of the center pixel in color plane i (e.g., R, G, and B) in noisy image. G'_{i_k} shows the gray values of the neighborhoods in the same color plane i in noisy texture image. In this respect, an unlike noise on centered pixel or its neighbors in one or two channels can't change the final pattern and extracted label. In other words, a neighbor pattern can be desired as 1 just when its intensity value is more than threshold (center value) in all of the color planes. In this respect, a new LBP representation can be defined for color textures with notation $NrCLBP_{P, R}$ as abbreviation of Noise-resistant Color Local binary patterns. For a colorful image in RGB, along with three previous extracted vectors, new feature vector can be extracted using $NrCLBP_{P,R}$. Finally, extracted vectors can be concatenated in a single representation as follows:

$$D = < D_H, \ D_R, \ D_G, \ D_B > \tag{13}$$

Where D_H shows the extracted feature vector based on $NrCLBP_{P,R}$.

Proposed surface defect detection approach

Any hole, damage, and abnormalities in surfaces are called defect. In this section, an approach is proposed for detecting defects in surfaces. The proposed approach has general theory, which is invariant with respect to texture descriptor type. It consists training phase and test phase.

Train phase

In this phase, first an image is taken from the surface that is defect less. Then texture analysis operator is applied over the whole image. In this article, NrCLBP is used as color/texture analysis operation. Then, regarding the Equation 13, one feature vector is extracted. This vector is called "Basic feature vector" and is marked by M.

Then the defect-less image is divided into windows of sizes W × W pixels. After that, the NrCLBP is applied over each of these windows. Thus, for each window, a feature vector is extracted. Next, non-similarity amount of

windows vector is computed through the basic feature vector (M) based on Log-likelihood ratios as follows:

$$\mathbf{L_i} = (S_i, M) = \sum_{k=1}^{L+1} S_{ki} \log\left(\frac{S_{ki}}{M_k}\right) i = 1, 2, \ldots, N \qquad (14)$$

Where "S_i" is the feature vector that was extracted for "i_{th}" window. M shows the basic feature vector. Also, N is the total number of windows, and "k" represents the "K_{th}" dimension of the feature vector.

Since minimization of Log-likelihood ratio shows the similarity to specific class. So, the maximum value among these ratios is regarded as the threshold for the defect-less window (Equation 15).

$$\mathbf{T} = \max(L_i) \ i = 1, 2, \ldots, N \qquad (15)$$

Where T is known as the defect-less threshold. "L_i" shows the non-similarity amount between "i_{th}" window and Basic vector (M).

Test phase

First, the test image is divided into windows of size W × W pixel. Then, for each window, the feature vector is extracted using NrCLBP. After that, for each of these windows, the log-likelihood ratio is computed as follows:

$$\mathbf{D_i} = (R_i, M) = \sum_{k=1}^{L+1} R_{ki} \log\left(\frac{R_{ki}}{M_k}\right) \ i = 1, 2, \ldots, N \qquad (16)$$

Where "R_i" is the feature vector that is computed for "i_{th} " window of test image. M is the basic vector. Also, N shows the total number of windows, and "k" represents the "k_{th}" dimension of the feature vector. After computing non-similarity ratio between test window vectors and basic vector, for each window, if any of these ratios is greater than the corresponding threshold, the window is declared as the defected window. It is shown in Equation 17.

$$\mathbf{i_{th}\ Window} = \begin{cases} \textit{Defected if } D_i > T \\ \textit{Non} - \textit{Defected otherwise} \end{cases} \qquad (17)$$

The output of the proposed approach is called "defect pattern" that is a binary image. Black pixels in the defect pattern represent defect-less areas of the surface, and white pixels represent defected areas.

Multi-resolution analysis

The proposed approach is a multi-resolution method. So, the results of choosing the different size of Neighborhood radius (R) in NrCLBP$_{P,R}$ can

be mixed by using the following equations, and it can be used for detecting the abnormalities in the surfaces. It is shown in the following equation:

$$L_i^Z = \sum_{z=1}^{Z} L_i\left(R_i^z, \ M_z\right) \tag{18}$$

Where Z is the number of $NrCLBP_{P,R}$ different sizes, and "i" corresponds to the "i_{th}" windows.

Experimental results

In this article, a general surface defect detection approach and a noise-resistant color/texture descriptor were proposed. To evaluate the effectiveness of our proposed approach, we carried out experiments on two surface datasets: architectonic stone (Tajeripour and Fekriershad 2014, 2012) and Fabric Textile (Bodnarova, Bennamoun, and Kubik 2000; Tajeripour, Kabir, and Sheikhi 2008).

The architectonic stone database (Tajeripour and Fekriershad 2014) contains 60 images in three categories known as "Non-Wavy Creamy Travertine," "Hatchet," and "Orange Travertine." Each category consists 20 images that were taken by a digital camera with resolution of 0.2 mm/pixel. Images are in different sizes that are collected under different illuminations and angles. The Patterned Fabric database (Tajeripour, Kabir, and Sheikhi 2008) contains three categories of patterned fabric textiles called "Dot-Pattern," "Star-Pattern," and "Box-Pattern." It was provided by Department of electronic and electric of Hong-Kong University. We selected randomly 20 images from each category to evaluate the experiment. Some examples of database images are shown in Figure 4.
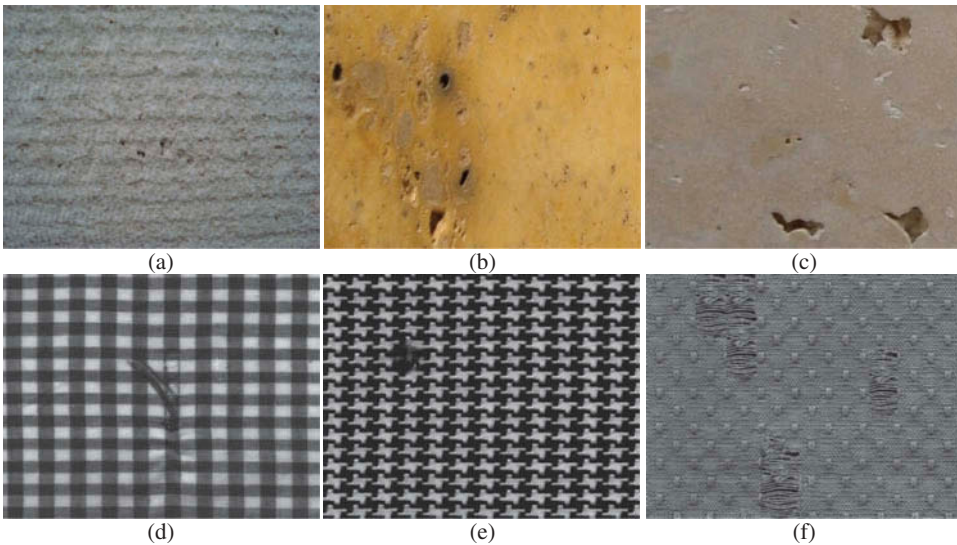
Figure 4. Some examples of database images.
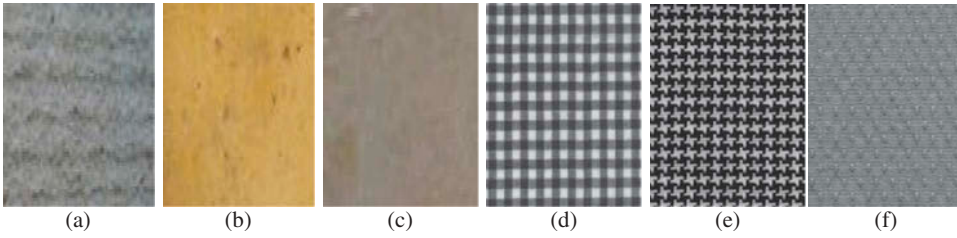
Figure 5. Train Defect-less samples (a) Hatchet Stone (b) Orange Travertine (c) Non-Wavy Creamy Travertine (d) Box-Pattern Fabric (e) Star-Pattern Fabric (f) Dot-Pattern Fabric.

First of all, one fully defect-less image of each category in size of 64×64 was provided for train phase. Train samples for each category are shown in Figure 5.

Next, the proposed approach based on different radius (R) and neighbors (P) of $NrCLBP_{P,R}$ was applied on database. One binary output defect pattern was provided for each test image. To evaluate performance, detection rate was used as follows. Detection rate is one of the popular criteria for measuring the performance of surface defect detection approaches (Bodnarova, Bennamoun, and Kubik 2000; Fekriershad and Tajeripour 2012; Tajeripour and Fekriershad 2014, 2012; Tajeripour, Kabir, and Sheikhi 2008).

$$\textbf{\textit{Detection Rate}} = 100 \times \frac{N_{RND} + N_{RD}}{N_{total}} \tag{19}$$

To measure the detection rate, the binary output defect pattern was divided to non-overlap windows by the sizes of $W \times W$ pixels, which is called "part" in this article. After that, each part that has at least one defected pixel was counted as a defected part. Different sizes were tested for windowing, and finally, size 16×16 was provided maximum detection rate in both the experiments.

In Equation 21, N_{RD} means the total number of parts that were really defected and also were detected as defect part. N_{RND} means the number of parts that were really defect-less and also were detected as defect-less part. For example, in Figure 6, an output binary defect pattern is shown where the first window (first column and first row) is categorized as non-defected part, and the fourth window (fourth column and first row) is categorized as defected part.

Detection accuracy results on stone database are shown in Table 1. Detection accuracy results on patterned fabric textile database are shown in Table 2. To evaluate performance accurately, specificity and sensitivity were computed for all of the defect patterns (Table 3).

$$\textbf{Specificity} = \frac{TN}{TN + FP} \tag{20}$$
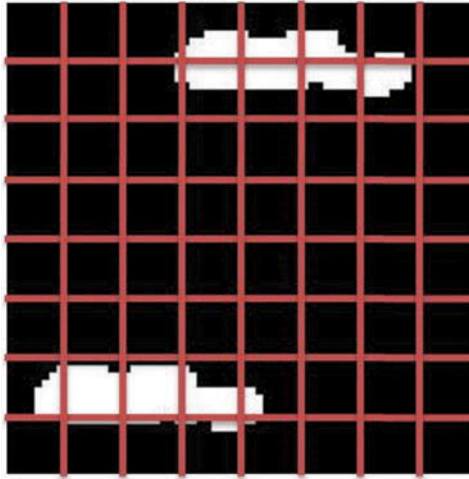
Figure 6. Determining result by defect detected image.

Table 1. The average of detection rate of applying multi-resolution LBP with different P and R, on stone database.

Features	Category Operation	Creamy Travertine	Hatchet	Orange Travertine
10	$NrCLBP_{8,1}$	93.47	92.24	90.33
18	$NrCLBP_{16,2}$	**96.2**	95.85	**95.90**
26	$NrCLBP_{24,3}$	90.42	91.39	95.82
10 + 18	$NrCLBP_{8,1} + NrCLBP_{16,2}$	93.60	94.47	93.71
10 + 26	$NrCLBP_{8,1} + NrCLBP_{24,3}$	92.37	95.70	92.64
18 + 26	$NrCLBP_{16,2} + NrCLBP_{24,3}$	90.53	**97.8**	93.15
10 + 18 + 26	$NrCLBP_{8,1} + NrCLBP_{16,2} + NrCLBP_{24,3}$	89.62	90.17	91.14

Table 2. The average of detection rate of applying multi-resolution LBP with different P & R on fabric textile database.

Features	Category Operation	Dot Pattern	Box Pattern	Star Pattern
10	$NrCLBP_{8,1}$	95.32	96.57	95.84
18	$NrCLBP_{16,2}$	96.18	**98.1**	**97.5**
26	$NrCLBP_{24,3}$	92.16	93.77	92.90
10 + 18	$NrCLBP_{8,1} + NrCLBP_{16,2}$	**97.5**	94.50	95.66
10 + 26	$NrCLBP_{8,1} + NrCLBP_{24,3}$	92.37	90.72	94.38
18 + 26	$NrCLBP_{16,2} + NrCLBP_{24,3}$	91.85	92.26	93.28
10 + 18 + 26	$NrCLBP_{8,1} + NrCLBP_{16,2} + NrCLBP_{24,3}$	90.18	90.37	91.06

Table 3. Specificity and Sensitivity of applying proposed approach on two databases.

Dataset	Architectonic Stone			Patterned Fabric		
Category Criteria	Creamy Travertine	Hatchet	Orange Travertine	Dot Pattern	Box Pattern	Star Pattern
Sensitivity	93.4	95.1	94.1	93.7	94.2	96.4
Specificity	96.7	96.9	96.8	98.1	98	97.7

$$\text{Sensitivity} = \frac{\text{TP}}{\text{TP} + \text{FN}} \qquad (21)$$

Where TP, TN, FP, and FN mean true positive, true negative, false positive, and false negative.

Comparison with state of the art

To compare effectiveness of our proposed NrCLBP, some efficient versions of LBP were evaluated as follows:

MBP was introduced in (Hafiane, Seetharaman, and Zavidovique 2007). In MBP, the median gray value of the neighborhood is used instead of center pixel threshold using the following definition:

$$MBP_{N,R}(x,y) = \sum_{k=0}^{P-1} \Omega(f_k - f_{median})2^k + \Omega(f_c - f_{median})2^P \qquad (22)$$

Where:

$$f_{median} = Median(\{f_0, f_1, \ldots, f_{P-1}, f_c\}) \qquad (23)$$

It provides local variance information along with local spatial structure together. Some overhead computation and noise sensitivity are disadvantages of MBP.

In the basic LBP and MLBP operator, selecting neighborhood in circular form is to make the algorithm invariant to rotation since during some applications, selecting circular neighborhood is not necessary. Also, computing brightness using interpolation in circular neighborhood needs a large amount of computations. Therefore, in 1DLBP (Fekriershad and Tajeripour 2012; Tajeripour and Fekriershad 2014), the neighborhood is a row (column) wise line segment. To apply 1DLBP, the gray value of the first pixel in the segment is compared with gray value of other pixels in the segment. In this version of LBP, the uniformity measure "U" corresponds to the number of spatial transitions (bitwise 0/1 changes) in the row (column) segment. The method of (Ngan and Pang 2006) uses Bollinger bands for detecting defects in patterned fabrics. Bollinger bands consist of three bands: upper, middle, and lower. In this method, patterned fabrics can be considered as comprising many rows (columns), with a pattern designed on each row (column). The principle of this method is that the patterned rows (columns) will generate periodic upper and lower bands. Any defect region in patterned fabric means that there would be a break of periodicity in the pattern. Also, MLBP, as it was described in section 'Modified local binary patterns (MLBP)', is applied on two databases. We used reported result in (Tajeripour and Fekriershad

Table 4. Comparison detection rate results (%) of state-of-the-art approaches on two datasets.

Dataset	Architecture Stone			Patterned Fabric Textile		
Category	Creamy		Orange	Dot	Box	Star
Operation	Travertine	Hatchet	Travertine	Pattern	Pattern	Pattern
Proposed NrCLBP	**96.2**	**97.3**	**95.90**	**97.2**	**98.1**	**97.5**
MLBP (Tajeripour, Kabir, and Sheikhi 2008)	93.67	94.11	95.43	96.5	97.6	97.4
1DLBP$_8$ (Tajeripour and Fekriershad 2014, Fekriershad and Tajeripour 2012)	95.60	96.22	95.74	96.6	97.8	96.8
MBP (Hafiane, Seetharaman, and Zavidovique 2007)	92.36	90.17	91.25	94.31	92	92.8
Bollinger Bands (Ngan and Pang 2006)	–	–	–	95.1	94.8	94.6

2014) on stone database using 1DLBP. Also, the reported result in (Fekriershad and Tajeripour 2012) on patterned fabric textile database using 1DLBP is shown in Table 4. Results in (Tajeripour, Kabir, and Sheikhi 2008) on fabric textile database using MLBP and Bollinger bands are used in Table 4. The standard proposed MBP in (Hafiane, Seetharaman, and Zavidovique 2007) is evaluated by us on two databases. In all experiments, the number of test set samples is same: 20 images in each category. Also, one really non-defected image was used as train set input.

As it is shown in Table 4, the proposed approach provides higher detection rate in comparison with previous versions of LBP and some state-of-the-art approaches on two database. Some examples of output binary defect patterns are shown in Figure 7.

Conclusion

In this article, a color/texture descriptor as a new version of LBP was proposed that is impulse noise resistant, multi-resolution, and rotation invariant. Then, a general surface defect detection algorithm was proposed that was invariant in respect of texture descriptor. Finally, proposed detection algorithm was evaluated using proposed NrCLBP. The experimental results have showed that the proposed approach has a high detection rate for much kind of surfaces. Some other advantages of this approach are as follows:

(I) Noise resistant, because of considering color plane information jointly
(II) Low computational complexity, because the base theory of proposed operation is approximately same to MLBP. Just one stage, AND logical combination, is added. This advantage makes our proposed approach useful in online applications.
(III) Generality and Usability, the proposed descriptor NrCLBP is a general color/texture descriptor that can be used in many image processing applications
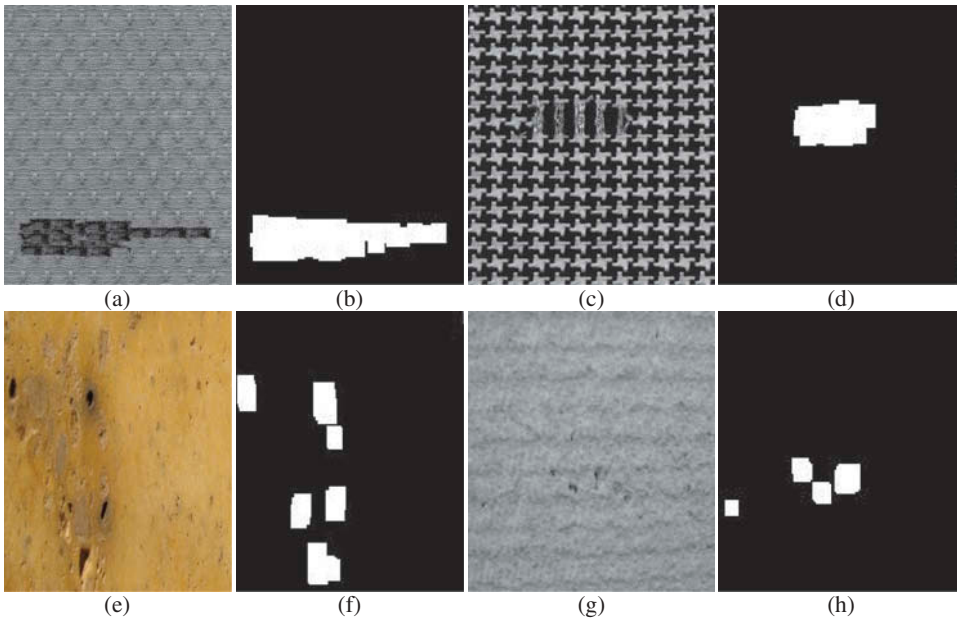
Figure 7. (a) Original image of Dot-pattern Fabric (b) defect pattern of (a) by NrCLBP$_{8,1}$ + NrCLBP$_{16,2}$ (c) Original image of Star-Pattern Fabric (d) defect pattern of (c) by NrCLBP$_{16,2}$ (e) Original image of Orange Travertine (f) defect pattern of (e) by NrCLBP$_{16,2}$ (g) Original image of Hatchet stone (h) defect pattern of (g) by NrCLBP$_{16,2}$ + NrCLBP$_{24,3}$.

References

Alimohamdi, H., and A. Ahmady. 2008. Detecting skin defect of fruits using optimal Gabor wavelet filter. *Proceedings of International Conference on Digital Image Processing* 2006:402–06.

Bodnarova, A., M. Bennamoun, and K. Kubik. 2000. Suitability analysis of techniques for flaw detection in textiles using texture analysis. *Pattern Analysis & Applications* 3:254–66. doi:10.1007/s100440070010.

Chan, C., and G. K. Pang. 2000. Fabric defect detection by Fourier analysis. *IEEE Transactions on Industry Applications* 36 (5):1267–76. doi:10.1109/28.871274.

Fekriershad, S. H., and F. Tajeripour. 2012. A robust approach for surface defect detection based on one dimensional local binary patterns. *Indian Journal of Science and Technology* 5 (8):3197–203.

Ghazini, M., A. Monadjemi, and K. Jamshidi. 2009. Defect detection of tiles using 2D Wavelet transform and statistical features. *World Academy of Science, Engineering &Technology* 49:901–04.

Hafiane, A., G. Seetharaman, and B. Zavidovique. 2007. Median binary pattern for textures classification. *Proceedings of the 4th International Conference* 4633:387–98.

Harinath, D., R. Babu, P. Satyanarayana, and M. V. Murthy. 2015. Defect detection in fabric using wavelet transform and genetics algorithms. *TMLAI Transactions on Machine Learning and Artificial Intelligence* 3 (6):10–18.

Henry, Y., K. Grantham, and H. Nelson. 2010. Ellipsoidal decision regions for motif-based patterned fabric defect detection. *Pattern Recognition* 43 (6):2132–44. doi:10.1016/j.patcog.2009.12.001.

Lin, C., and C. Yu-Yeh. 2009. Texture defect detection system with image deflection compensation. *WSEAS Transactions on Computers* 8 (9):1575–86.

Ngan, H. Y. T., and G. K. H. Pang. 2006. Novel method for patterned fabric inspection using Bollinger bands. *Optical Engineering* 45 (8):1–15.

Ojala, T., T. Maeenpaeae, and M. Pietikaeinen. 2000. Texture classification by multi predicate local binary pattern operators. *Proceedings of 15th International Conference on Pattern Recognition* 3:951–54.

Ojala, T., M. Pietikainen, and T. Maenpaa. 2002. Multi resolution gray-scale and rotation invariant texture classification with local binary patterns. *IEEE Transactions on Pattern Analysis and Machine Intelligence* 24 (7):971–87. doi:10.1109/TPAMI.2002.1017623.

Pietikäinen, M., T. Ojala, and Z. Xu. 2000. Rotation-invariant texture classification using feature distributions. *Pattern Recognition* 33:43–52. doi:10.1016/S0031-3203(99)00032-1.

Tajeripour, F., and S. H. Fekriershad. 2012. Porosity detection by using improved local binary pattern. *Proceedings of the 11th WSEAS International Conference on Signalling Processing, Robotics and Automation (ISPRA '12)* 116–21.

Tajeripour, F., and S. H. Fekriershad. 2014. Developing a novel approach for stone porosity computing using modified local binary patterns and single scale retinex. *Arabian Journal for Science and Engineering* 39 (2):875–89. doi:10.1007/s13369-013-0725-8.

Tajeripour, F., E. Kabir, and A. Sheikhi. 2008. Fabric defect detection using modified local binary patterns. *EURASIP Journal on Advances in Signal Processing* 8:1–12.

Tan, X., and B. Triggs. 2010. Enhanced local texture feature set for face recognition under different lighting conditions. *IEEE Transaction on Image Processing* 19 (6):1635–50. doi:10.1109/TIP.2010.2042645.

Tolba, A. S. 2011. Fast defect detection in homogeneous flat surface products. *Expert Systems with Applications: an International Journal* 38 (10):12339–47. doi:10.1016/j.eswa.2011.04.012.

Xie, X. 2008. A review of recent advances in surface defect detection using texture analysis. *Electronic Letters on Computer Vision and Image Analysis* 7 (3):1–22.

Yuan, X., L. Wu, and Q. Peng. 2015. An improved otsu method using weighted object variance for defect detection. *Applied Surface Science* 349:472–84. doi:10.1016/j.apsusc.2015.05.033.